Nucleon Vector and Axial-vector Form Factors

Tanmoy Bhattacharya[1], Rajan Gupta[1],
Yong-Chull Jang[1], Huey-Wen Lin[3], Boram Yoon[2]

Theoretical Division T-2[1],
Los Alamos National Laboratory, Los Alamos, New Mexico 87545, USA

Computer, Computational, Statistical Science Division CCS-7[2],
Los Alamos National Laboratory, Los Alamos, New Mexico 87545, USA

Department of Physics and Astronomy, Michigan State University[3],
East Lansing, Michigan 48824, USA

34th International Symposium on Lattice Field Theory, 24–30 July 2016

Collaborators

Clover-on-HISQ
(PNDME Collaboration)

Tanmoy Bhattacharya,
Rajan Gupta, Huey-Wen Lin,
Boram Yoon

Clover-on-Clover
(NME Collaboration)

Tanmoy Bhattacharya,
Rajan Gupta, Huey-Wen Lin,
Boram Yoon, Jeremy Green,
Balint Joo, Kostas Orginos,
David Richards, Sergey Syritsyn,
Frank Winter

Allocations at NERSC,
USQCD-Fermilab, LANL

ALCC allocation on TITAN at
OLCF

Vector and Axial-vector Form Factors

$$\left\langle N(\vec{p}_f)|V_\mu(\vec{Q})|N(\vec{p}_i)\right\rangle = \overline{u}_N(\vec{p}_f)\left[\gamma_\mu F_1(Q^2) + \sigma_{\mu\nu}Q_\mu\frac{F_2(Q^2)}{2M_N}\right]u_N(\vec{p}_i)$$

$$\left\langle N(\vec{p}_f)|A_\mu(\vec{Q})|N(\vec{p}_i)\right\rangle = \overline{u}_N(\vec{p}_f)\left[\gamma_\mu G_A(Q^2) + Q_\nu\frac{G_P(Q^2)}{2M_N}\right]\gamma_5 u_N(\vec{p}_i)$$

$$G_E(Q^2) = F_1(Q^2) - \frac{Q^2}{4M_N^2}F_2(Q^2)$$

$$G_M(Q^2) = F_1(Q^2) + F_2(Q^2)$$

Nucleon Charge Radii

$$\langle r^2_{E,M} \rangle = -6 \frac{d}{dQ^2} \left(\frac{G^v_{E,M}(Q^2)}{G^v_{E,M}(0)} \right) \Bigg|_{Q^2=0}$$

$$\langle r^2_{1,2} \rangle = -6 \frac{d}{dQ^2} \left(\frac{F^v_{1,2}(Q^2)}{F^v_{1,2}(0)} \right) \Bigg|_{Q^2=0}$$

$$\langle r^2_{A,P} \rangle = -6 \frac{d}{dQ^2} \left(\frac{G^v_{A,P}(Q^2)}{G^v_{A,P}(0)} \right) \Bigg|_{Q^2=0}$$

r_E [fm]	r_M [fm]	Note	Ref.
$0.84^{+0.01}_{-0.01}$	$0.86^{+0.02}_{-0.03}$	p	T. Lorenz *et. al.*, Eur. Phys. J. A (2012) 48: 151

Ensembles

- HISQ

Ensemble ID	a (fm)	$M_\pi^{\rm sea}$ (MeV)	$L^3 \times T$	$M_\pi^{\rm val} L$	$N_{\rm conf}$	$N_{\rm meas}^{\rm HP}$	$N_{\rm meas}^{\rm AMA}$
a12m310	0.1207(11)	305.3(4)	$24^3 \times 64$	4.55	1013	8104	64832
a12m220L	0.1189(09)	217.0(2)	$40^3 \times 64$	5.49	1010	8080	68680
a09m310	0.0888(08)	312.7(6)	$32^3 \times 96$	4.51	881	7048	
a09m220	0.0872(07)	220.3(2)	$48^3 \times 96$	4.79	890	7120	
a09m130	0.0871(06)	128.2(1)	$64^3 \times 96$	3.90	883	7064	84768
a06m310	0.0582(04)	319.3(5)	$48^3 \times 144$	4.52	1000	8000	64000
a06m220	0.0578(04)	229.2(4)	$64^3 \times 144$	4.41	650	2600	41600

- Clover

Ensemble ID	a (fm)	$M_\pi^{\rm sea}$ (MeV)	$L^3 \times T$	$M_\pi^{\rm val} L$	$N_{\rm conf}$	$N_{\rm meas}^{\rm HP}$	$N_{\rm meas}^{\rm AMA}$
a114m315	0.114(1)	316(3)	$32^3 \times 96$	5.55	1000	4020	128480
a081m315	0.081(1)	312(3)	$32^3 \times 64$	4.08	1005	3015	96480
a079m195	0.079(1)	192(2)	$48^3 \times 96$	4.09	629	2516	80512
a079m195L	0.079(1)	198(6)	$64^3 \times 128$	5.46	467	2335	74720

Error and Cost Reduction Techniques

- Truncated Solver with Bias Correction (AMA)

  [G. S. Bali et. al., Comput. Phys. Commun. 181 (2010) 1570–1583]

  [T. Blum et. al., Phys. Rev. D88 (2013) no.9, 094503]

- Coherent Source Sequential Propagator Method

- Covariant Gaussian Source Smearing

- Two-states Fit to multiple t_{sep} to get $t_{\text{sep}} \to \infty$ value

2-states Fits

$$C_\Gamma^{(2\mathrm{pt})}(t,\boldsymbol{p}) = |\mathcal{A}_0|^2 e^{-E_0 t} + |\mathcal{A}_1|^2 e^{-E_1 t}$$

$$C_\Gamma^{(3\mathrm{pt})}(t;\tau;\boldsymbol{p}',\boldsymbol{p}) = |\mathcal{A}_0'||\mathcal{A}_0|\langle 0'|\mathcal{O}_\Gamma|0\rangle e^{-E_0 t - M_0(\tau-t)} + |\mathcal{A}_1'||\mathcal{A}_1|\langle 1'|\mathcal{O}_\Gamma|1\rangle e^{-E_1 t - M_1(\tau-t)}$$
$$+ |\mathcal{A}_0'||\mathcal{A}_1|\langle 0'|\mathcal{O}_\Gamma|1\rangle e^{-E_0 t - M_1(\tau-t)} + |\mathcal{A}_1'||\mathcal{A}_0|\langle 1'|\mathcal{O}_\Gamma|0\rangle e^{-E_1 t - M_0(\tau-t)}$$

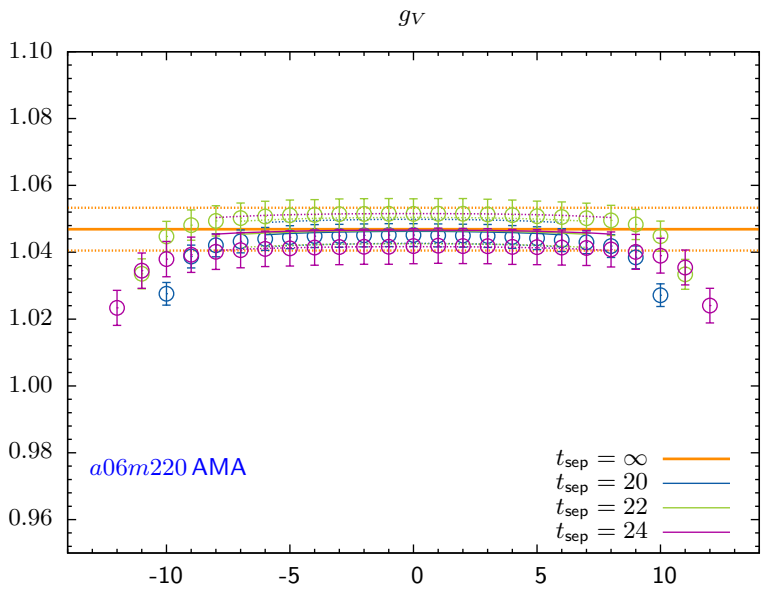

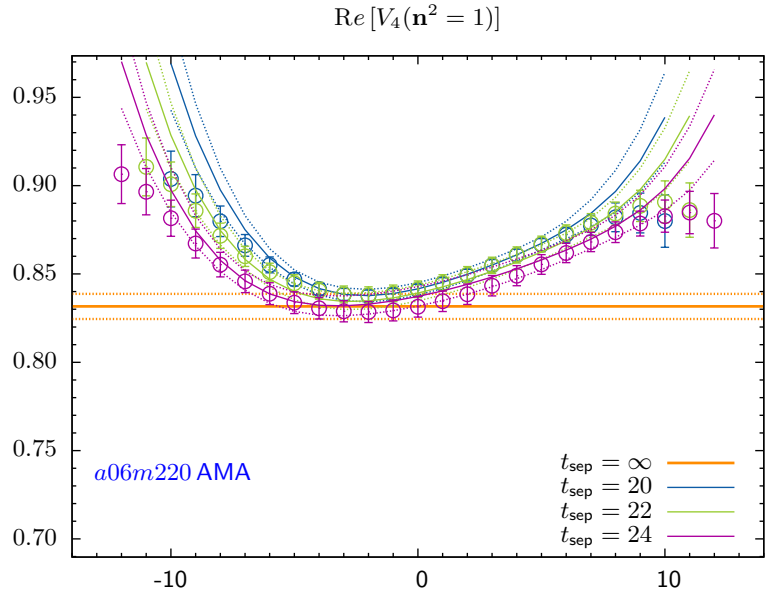

- For plotting data we use the ratios (the fits are 2-state)

$$\frac{C_\Gamma^{(3\mathrm{pt})}(t,\tau)}{C_2^{\mathrm{fit}}(\tau)} \qquad \frac{C_\Gamma^{(3\mathrm{pt})}(t,\tau;\boldsymbol{p}',\boldsymbol{p})}{C_2(\tau,\boldsymbol{p}')}\left[\frac{C_2(t,\boldsymbol{p}')C_2(\tau,\boldsymbol{p}')C_2(\tau-t,\boldsymbol{p})}{C_2(t,\boldsymbol{p})C_2(\tau,\boldsymbol{p})C_2(\tau-t,\boldsymbol{p}')}\right]^{1/2}$$

Phenomenological Fits

- Kelly Parameterization: $\tau = Q^2/4M^2, X = \{Ep, Mp, Mn\}$

$$G_X(Q^2) = G(0)\frac{\sum_{k=0}^{n} a_k \tau^k}{1 + \sum_{k=1}^{n+2} b_k \tau^k}\,,\; G_{En}(Q^2) = \frac{A\tau}{1 + B\tau}\frac{1}{\left(1 + Q^2/0.71\mathrm{GeV}^2\right)^2}$$

- Dipole for G_E, G_M, G_A:

$$G(Q^2) = \frac{G(0)}{\left(1 + Q^2/M^2\right)^2}\,,\; G_{E,A}(0) = 1\,, G_M(0) = \mu = 1 + \kappa\,, \langle r^2 \rangle = \frac{12}{M^2}$$

- Dipole with pion-pole for G_P:

$$G(Q^2) = \frac{1}{\left(1 + Q^2/M^2\right)^2}\frac{4M^2_{p,\mathrm{phys}}}{Q^2 + M^2_{\pi,\mathrm{phys}}}$$

G_E

Clover-on-HISQ

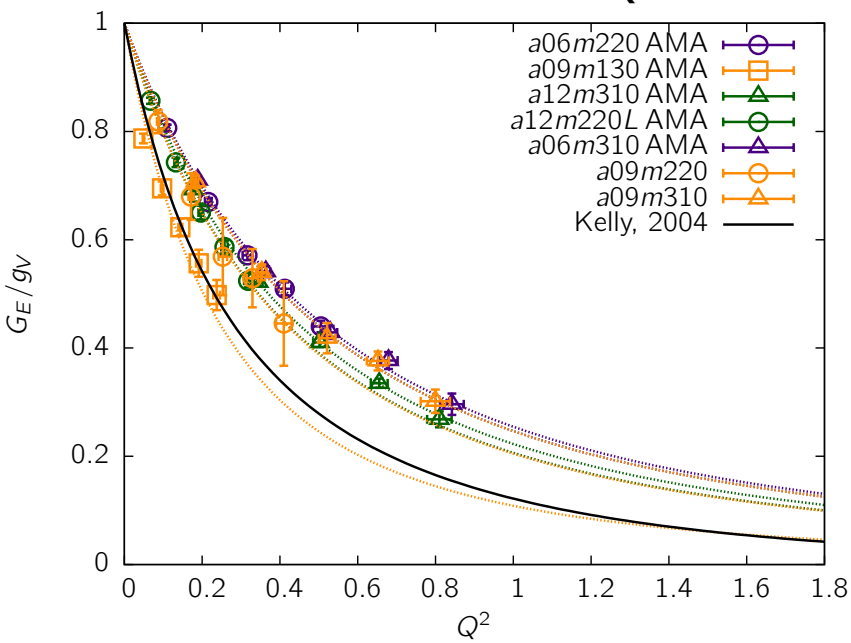

Clover-on-Clover

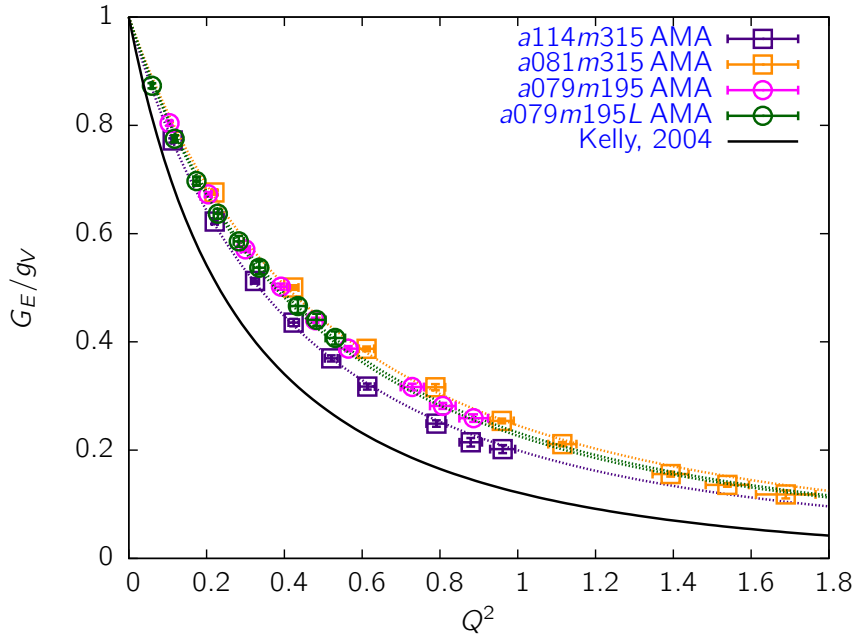

G_E

Clover-on-HISQ

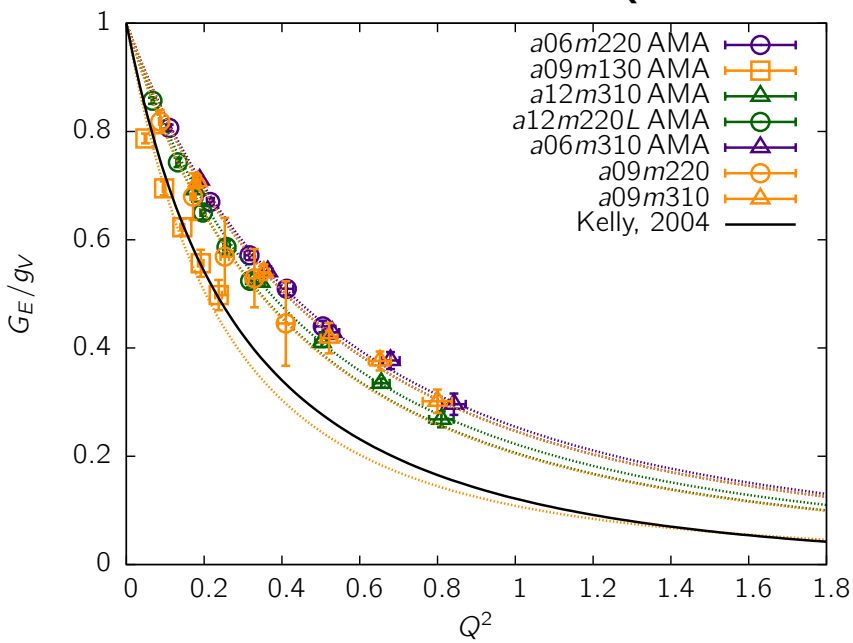

Clover-on-Clover

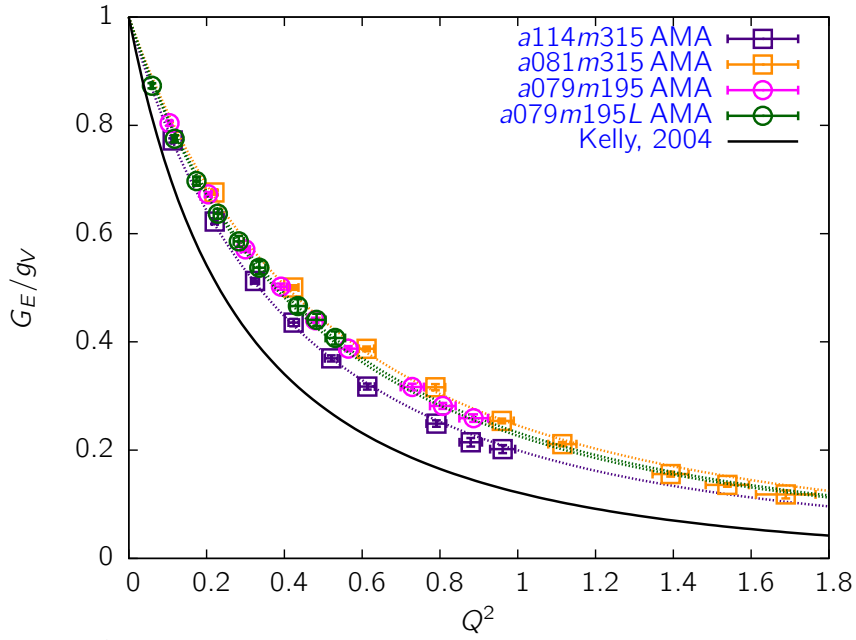

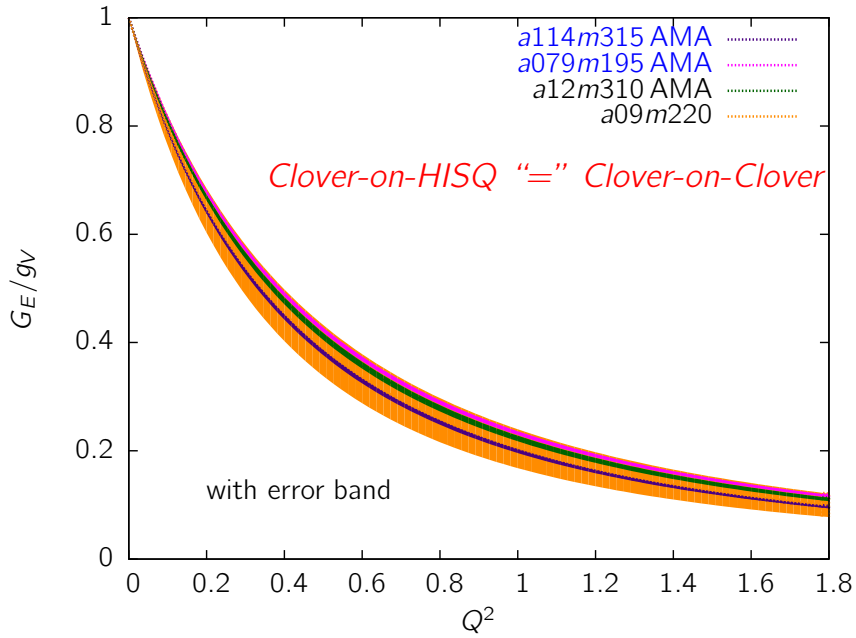

G_M

Clover-on-HISQ

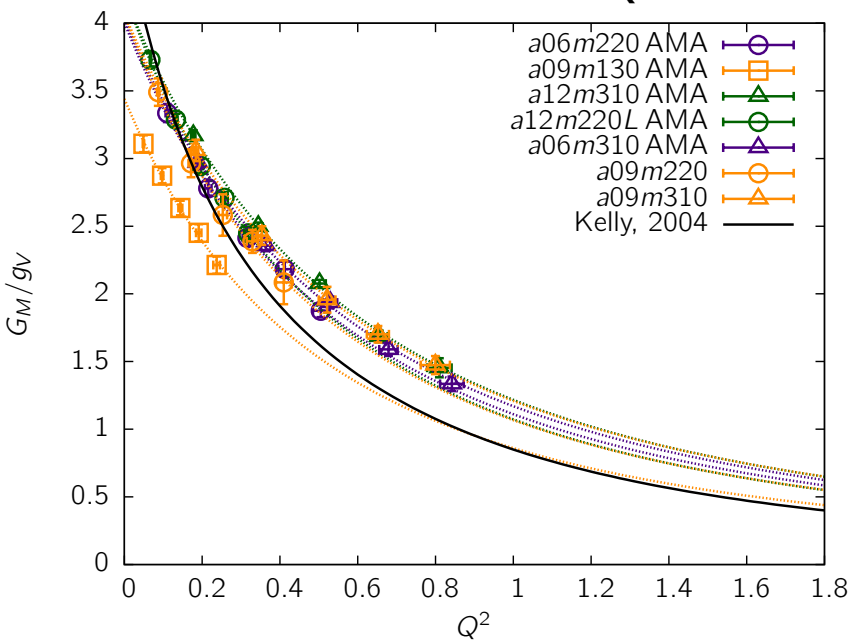

Clover-on-Clover

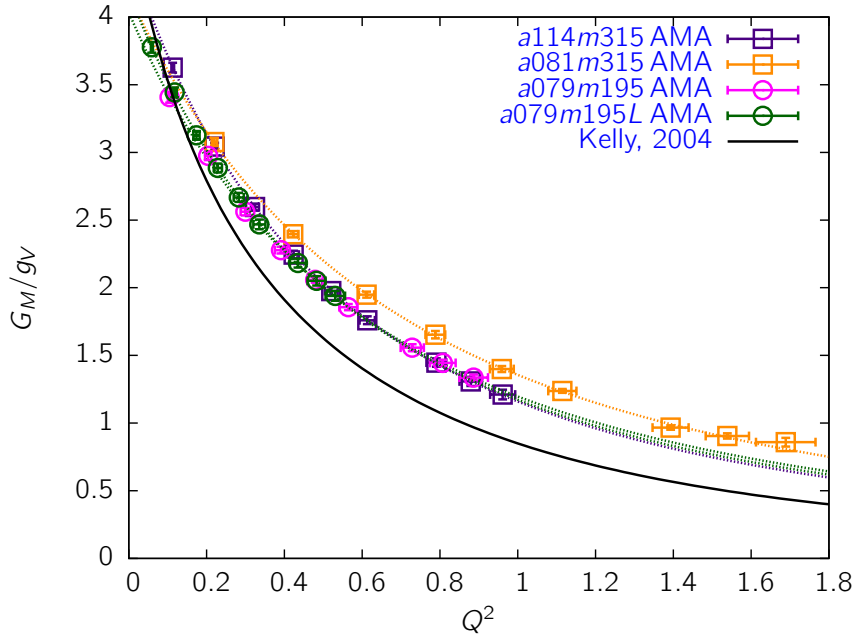

G_M

Clover-on-HISQ

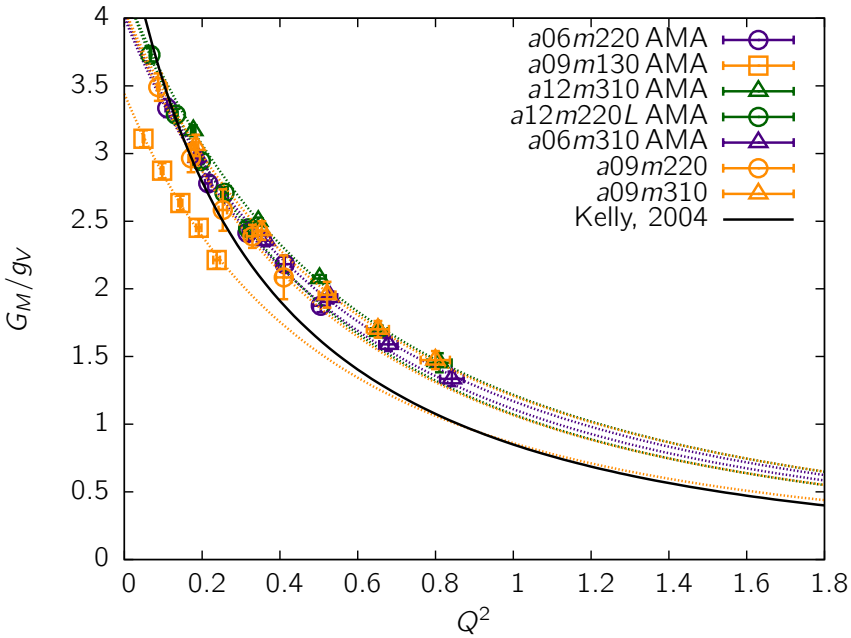

Clover-on-Clover

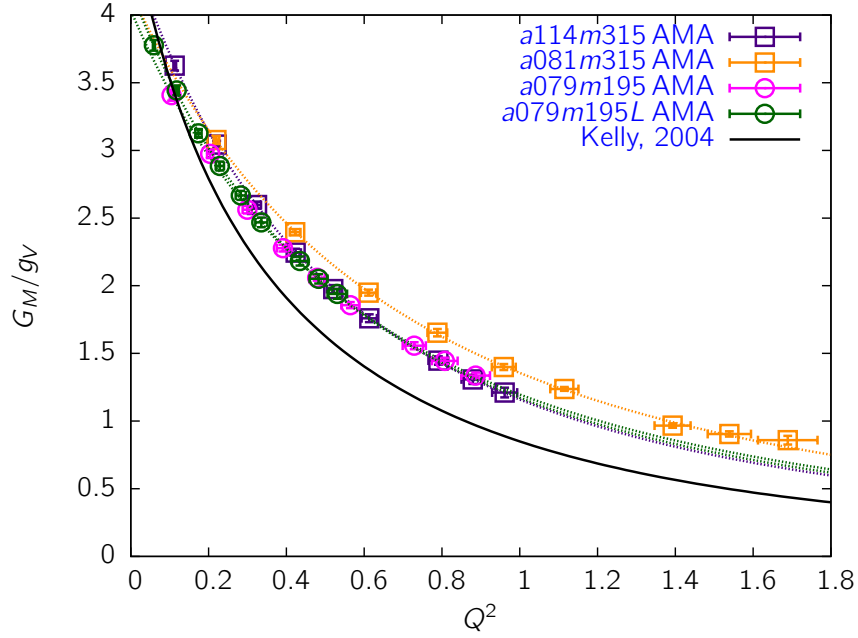

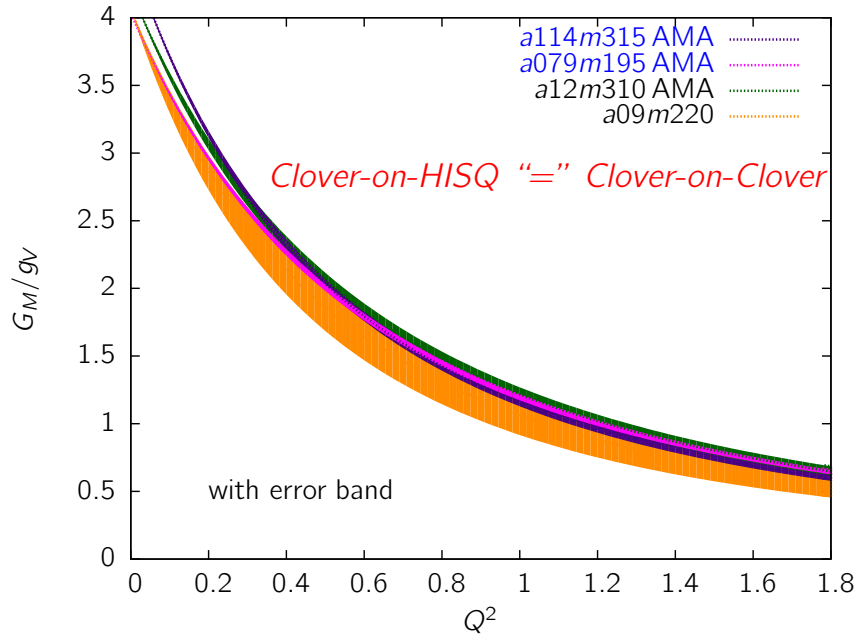

$\mu G_E / G_M$

Clover-on-HISQ

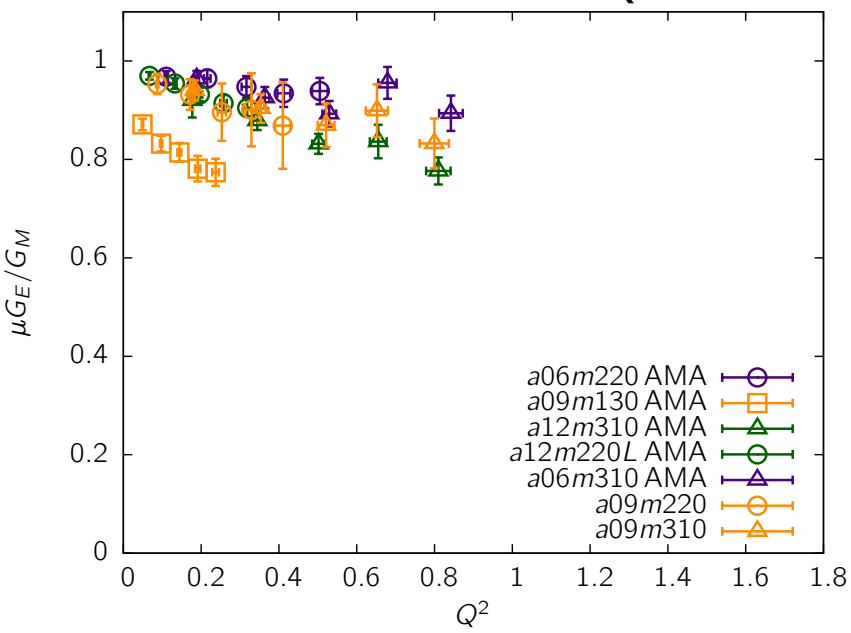

Clover-on-Clover

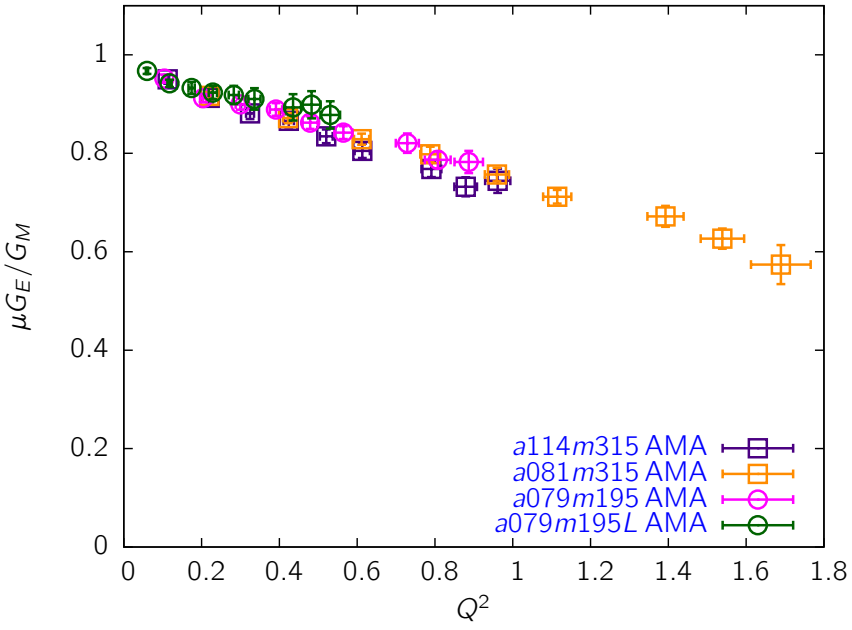

$\mu G_E / G_M$

Clover-on-HISQ

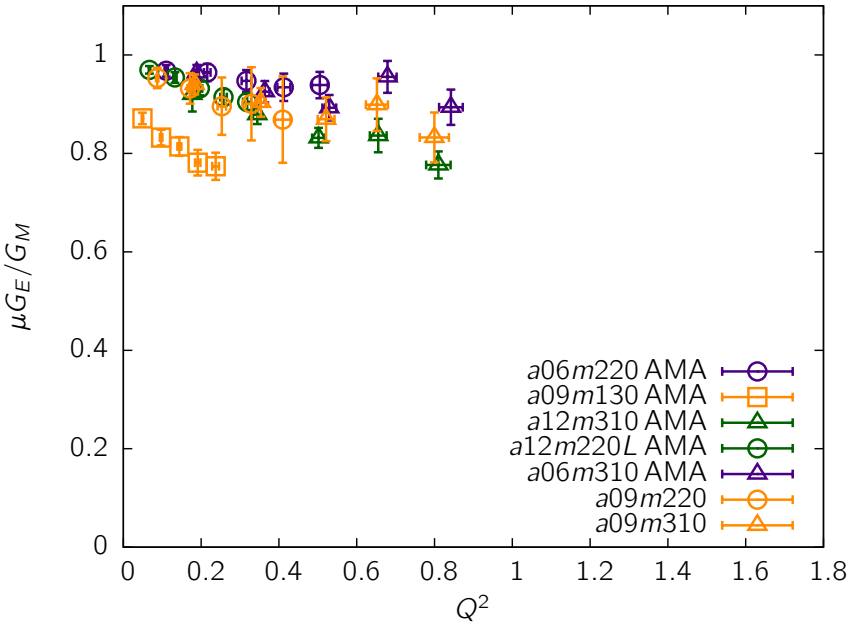

Clover-on-Clover

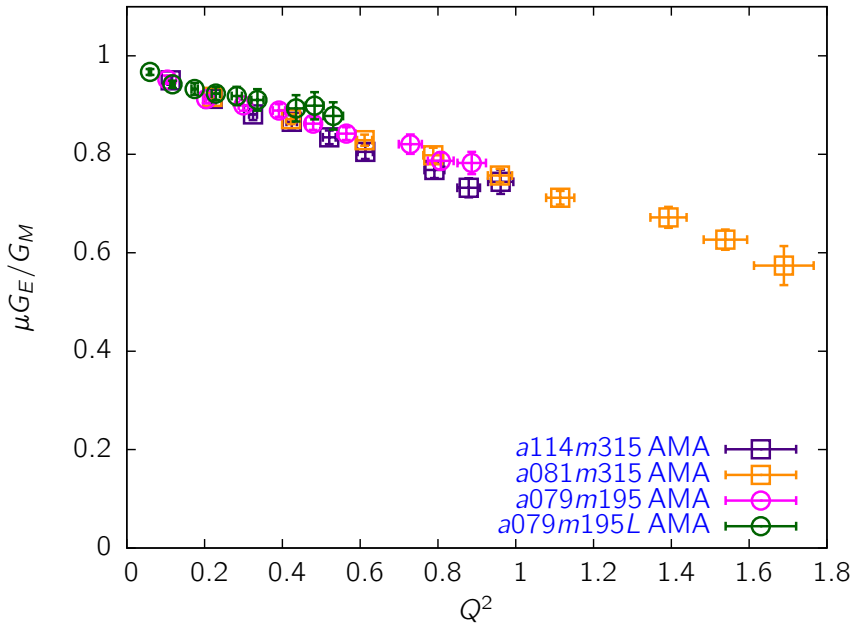

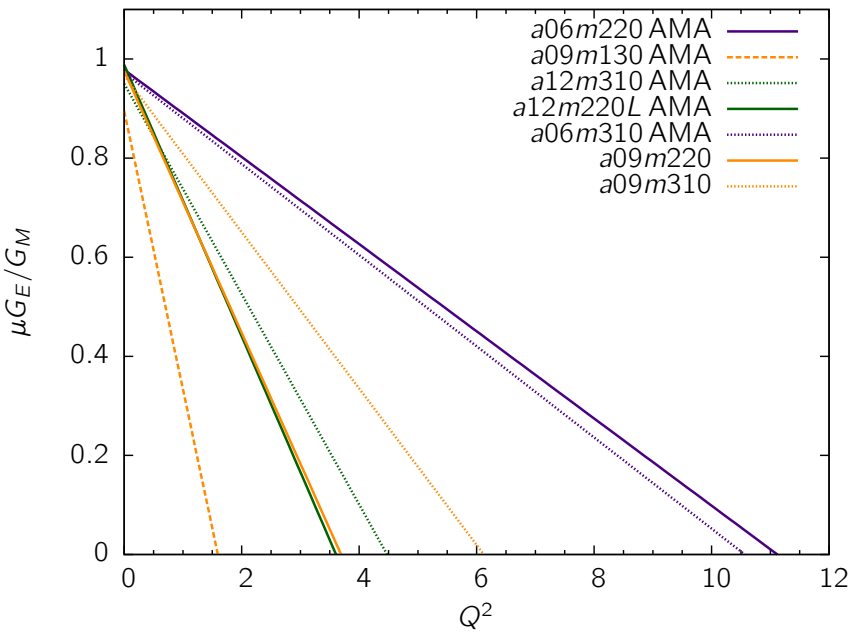

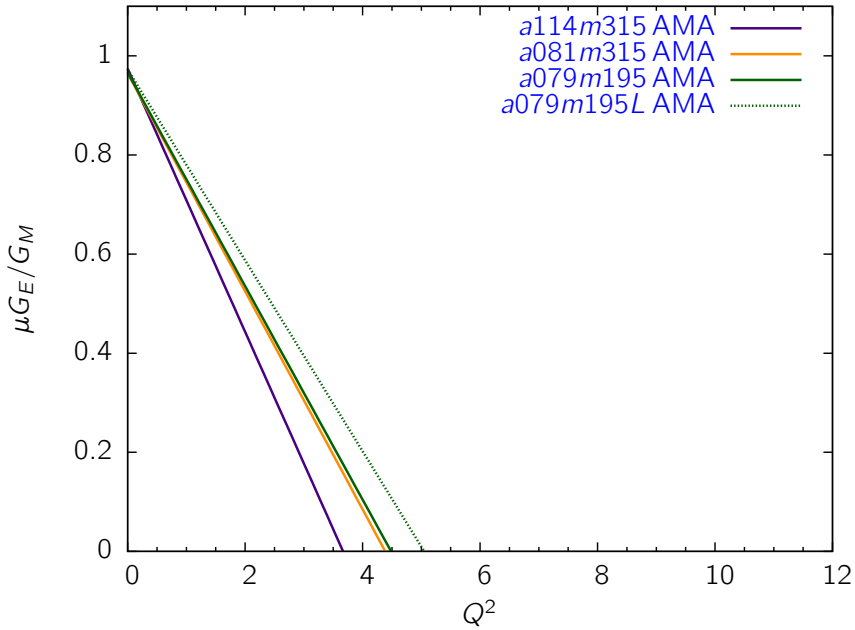

G_A

Clover-on-HISQ

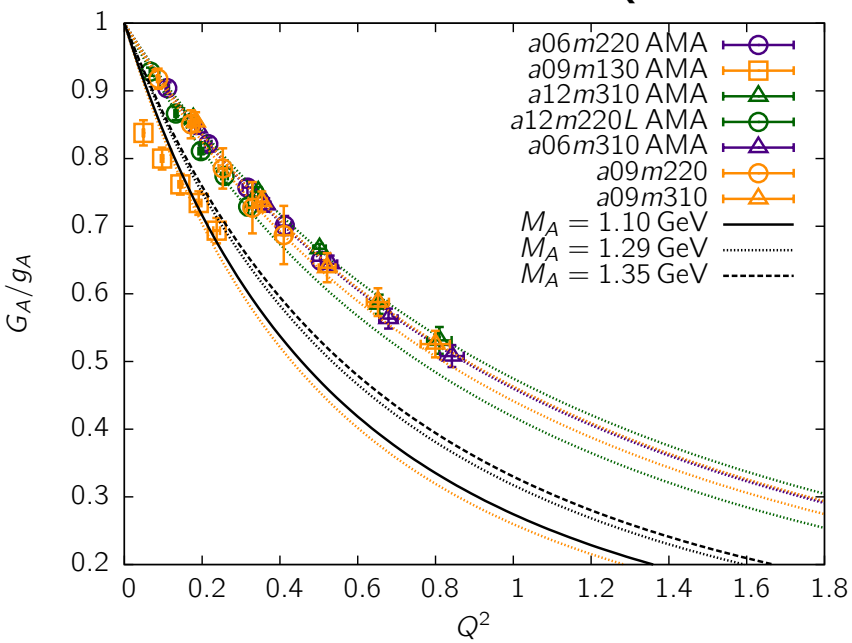

Clover-on-Clover

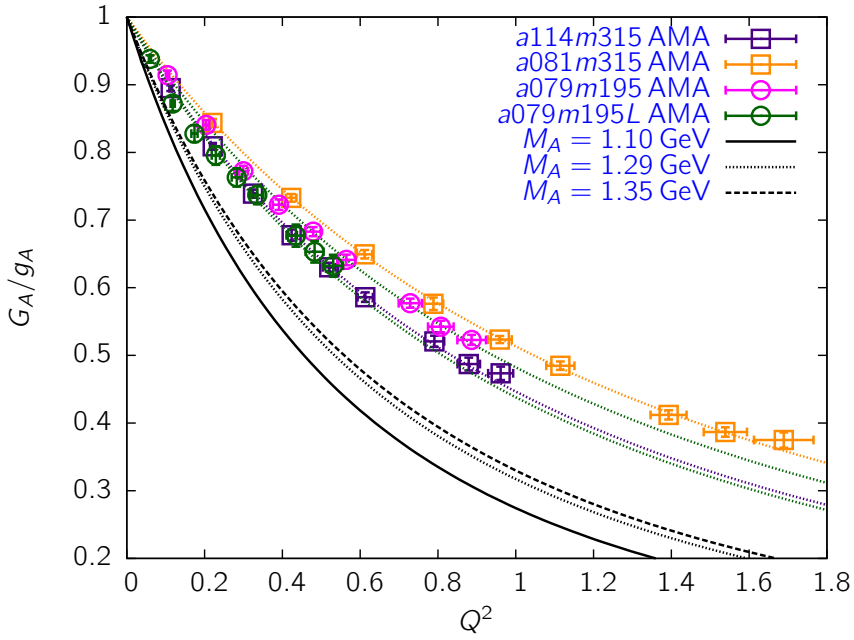

G_A

Clover-on-HISQ

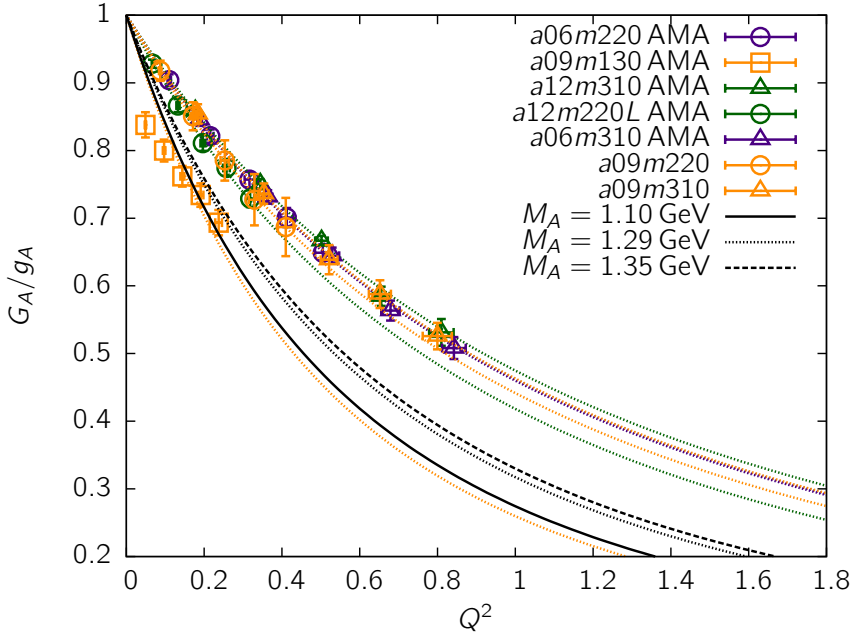

Clover-on-Clover

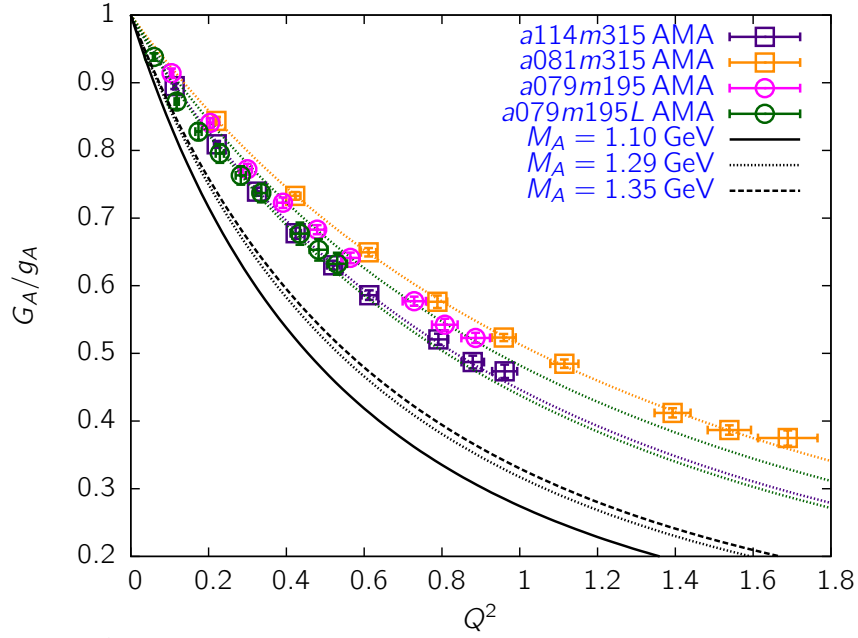

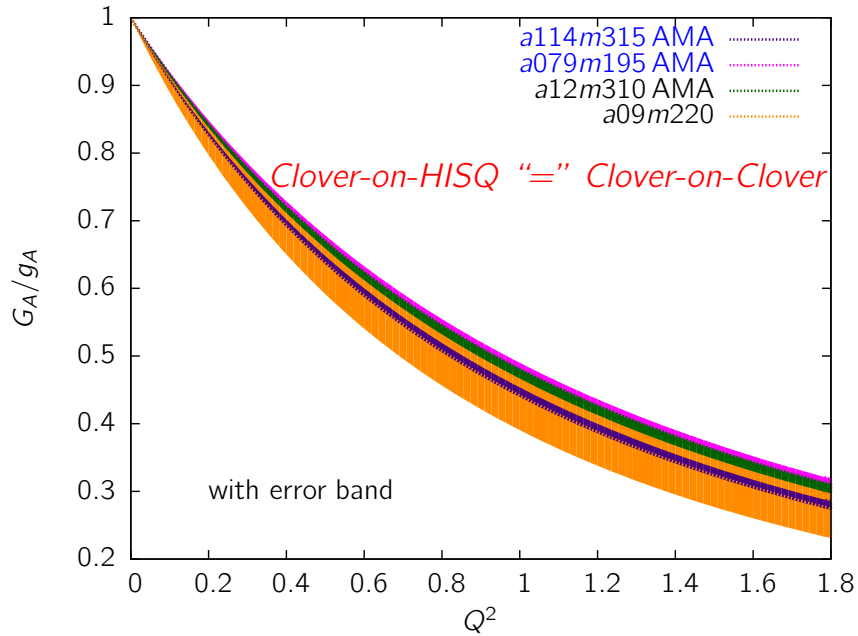

G_P

Clover-on-HISQ

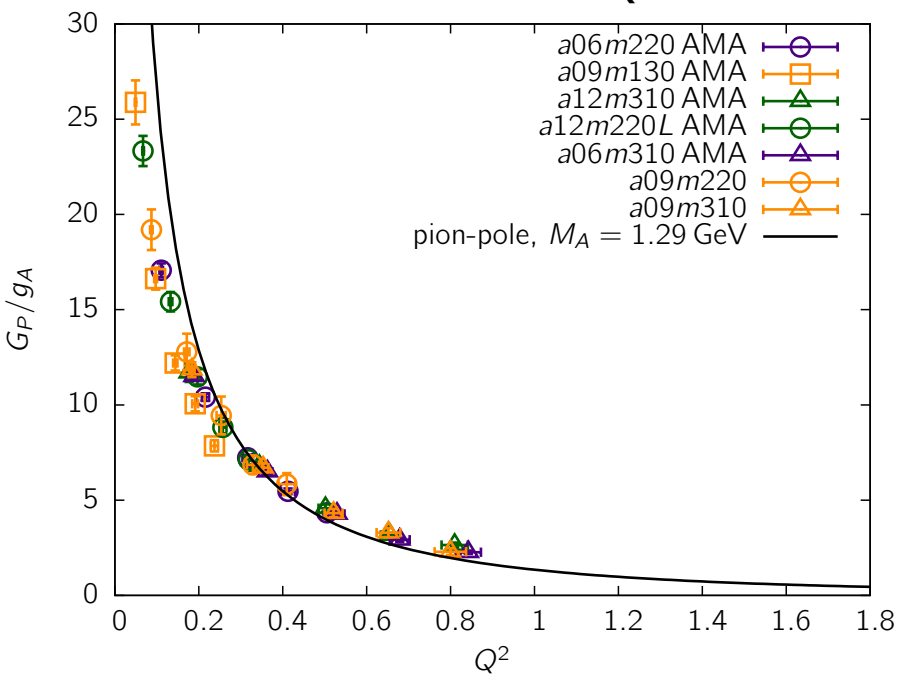

Clover-on-Clover

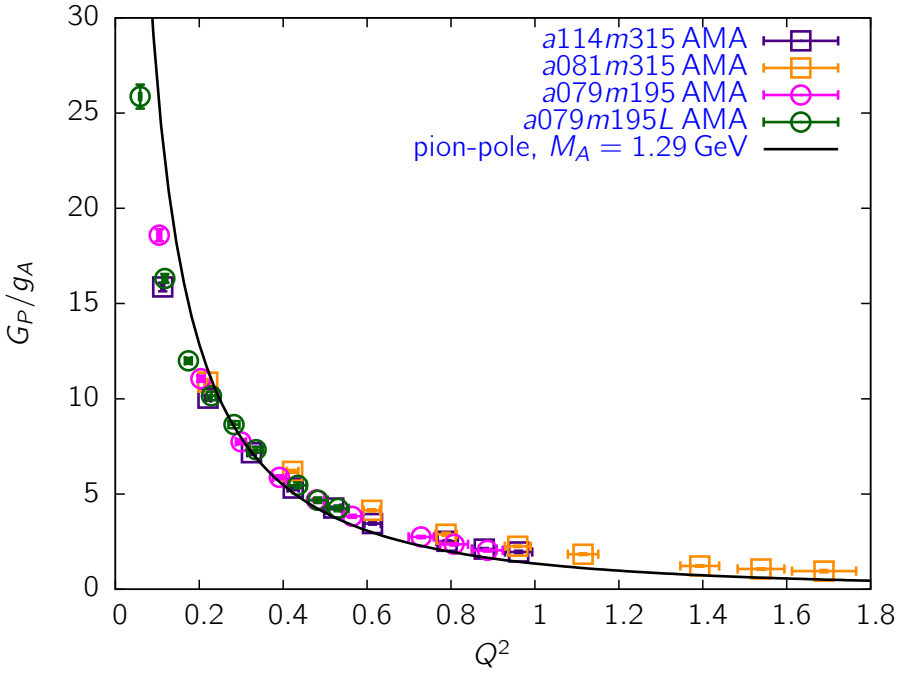

Q^2-dependence: Dipole Fit

- Clover-on-HISQ

	M_E [GeV]	$< r_E^2 >$ [fm^2]	χ_E^2/DOF	M_M	$< r_M^2 >$	κ	χ_M^2/DOF	M_A	$< r_A^2 >$	χ_A^2/DOF
a12m310 AMA	0.945(10)	0.523(11)	0.08(1)	1.078(25)	0.402(19)	3.210(93)	0.35(2)	1.489(20)	0.211(11)	0.20(1)
a12m220L AMA	0.912(17)	0.561(21)	0.052(4)	1.008(22)	0.459(21)	3.222(63)	0.153(8)	1.353(42)	0.255(21)	0.166(8)
a09m310	0.993(25)	0.474(24)	0.23(1)	1.095(32)	0.400(23)	3.07(12)	0.018(2)	1.460(49)	0.219(24)	0.086(7)
a09m220	0.909(73)	0.565(91)	0.05(1)	1.024(71)	0.445(62)	3.07(17)	0.12(1)	1.41(11)	0.236(91)	0.019(2)
a09m130 AMA	0.701(20)	0.951(53)	6.57(6)	1.000(46)	0.467(43)	2.441(82)	0.16(1)	1.019(40)	0.450(53)	5.83(8)
a06m310 AMA	1.009(17)	0.459(15)	0.37(2)	1.081(25)	0.400(19)	3.031(90)	0.26(1)	1.456(32)	0.220(15)	0.20(1)
a06m220 AMA	0.993(15)	0.474(14)	0.41(2)	1.055(24)	0.420(19)	3.004(91)	0.38(1)	1.451(38)	0.222(14)	0.020(3)

- Clover-on-Clover

	M_E [GeV]	$< r_E^2 >$ [fm^2]	χ_E^2/DOF	M_M	$< r_M^2 >$	κ	χ_M^2/DOF	M_A	$< r_A^2 >$	χ_A^2/DOF
a114m315 AMA	0.899(8)	0.578(10)	1.12(3)	1.020(14)	0.449(12)	3.462(53)	0.042(2)	1.419(17)	0.232(10)	0.52(2)
a081m315 AMA	0.991(6)	0.476(6)	6.77(7)	1.152(10)	0.352(6)	3.172(51)	0.77(2)	1.589(14)	0.185(6)	0.41(1)
a079m195 AMA	0.965(7)	0.502(8)	0.50(1)	1.093(12)	0.391(8)	3.035(51)	0.24(1)	1.508(20)	0.205(8)	0.32(1)
a079m195L AMA	0.953(16)	0.515(17)	0.99(3)	1.061(20)	0.415(16)	3.184(55)	0.069(3)	1.399(48)	0.239(17)	0.81(2)

Q^2-dependence: Dipole Fit

- Clover-on-HISQ

	M_E [GeV]	$< r_E^2 >$ [fm^2]	χ_E^2/DOF	M_M	$< r_M^2 >$	κ	χ_M^2/DOF	M_A	$< r_A^2 >$	χ_A^2/DOF
a12m310 AMA	0.945(10)	0.523(11)	0.08(1)	1.078(25)	0.402(19)	3.210(93)	0.35(2)	1.489(20)	0.211(11)	0.20(1)
a12m220L AMA	0.912(17)	0.561(21)	0.052(4)	1.008(22)	0.459(21)	3.222(63)	0.153(8)	1.353(42)	0.255(21)	0.166(8)
a09m310	0.993(25)	0.474(24)	0.23(1)	1.095(32)	0.400(23)	3.07(12)	0.018(2)	1.460(49)	0.219(24)	0.086(7)
a09m220	0.909(73)	0.565(91)	0.05(1)	1.024(71)	0.445(62)	3.07(17)	0.12(1)	1.41(11)	0.236(91)	0.019(2)
a09m130 AMA	0.701(20)	0.951(53)	6.57(6)	1.000(46)	0.467(43)	2.441(82)	0.16(1)	1.019(40)	0.450(53)	5.83(8)
a06m310 AMA	1.009(17)	0.459(15)	0.37(2)	1.081(25)	0.400(19)	3.031(90)	0.26(1)	1.456(32)	0.220(15)	0.20(1)
a06m220 AMA	0.993(15)	0.474(14)	0.41(2)	1.055(24)	0.420(19)	3.004(91)	0.38(1)	1.451(38)	0.222(14)	0.020(3)

- Clover-on-Clover

	M_E [GeV]	$< r_E^2 >$ [fm^2]	χ_E^2/DOF	M_M	$< r_M^2 >$	κ	χ_M^2/DOF	M_A	$< r_A^2 >$	χ_A^2/DOF
a114m315 AMA	0.899(8)	0.578(10)	1.12(3)	1.020(14)	0.449(12)	3.462(53)	0.042(2)	1.419(17)	0.232(10)	0.52(2)
a081m315 AMA	0.991(6)	0.476(6)	6.77(7)	1.152(10)	0.352(6)	3.172(51)	0.77(2)	1.589(14)	0.185(6)	0.41(1)
a079m195 AMA	0.965(7)	0.502(8)	0.50(1)	1.093(12)	0.391(8)	3.035(51)	0.24(1)	1.508(20)	0.205(8)	0.32(1)
a079m195L AMA	0.953(16)	0.515(17)	0.99(3)	1.061(20)	0.415(16)	3.184(55)	0.069(3)	1.399(48)	0.239(17)	0.81(2)

Summary

- Clover-on-HISQ and Clover-on-Clover agree
- Dipole ansatz works well except
  - G_E, G_A from a09m130 (HISQ)
  - G_E from a081m315 (Clover)

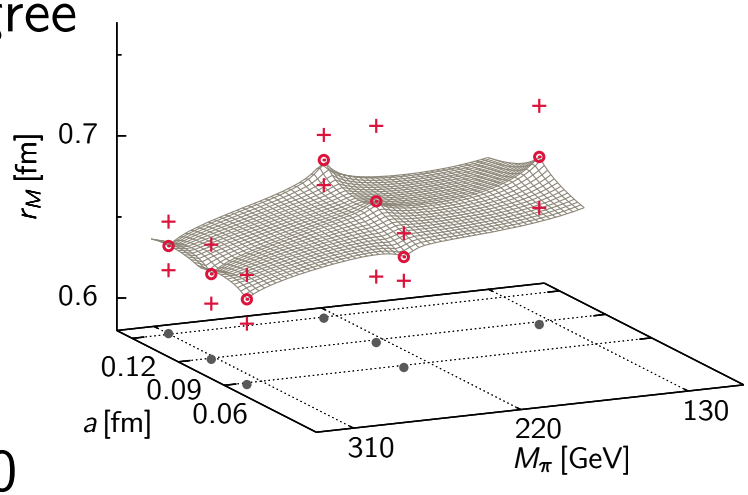

- Fixed a: charge radii increase as $M_\pi \to 0$
- Fixed M_π: charge radii decrease as $a \to 0$
  - For r_M and r_A: dependence on a is small
- Overall trend: charge radii increases as $a \to 0$ and $M_\pi \to 135$ MeV
- Physical mass a09m130 ensemble needs further analysis